

# Broadband and polarization-independent beam steering using dielectrophoresis-tilted prism

Yeong-Jyh Lin, Kuan-Ming Chen, and Shin-Tson Wu\*

College of Optics and Photonics, University of Central Florida, Orlando, Florida 32816, USA

\*swu@mail.ucf.edu

**Abstract:** A broadband beam steering device using the dielectrophoresis-tilted prism of liquids is demonstrated. Dielectric force is utilized to slant the interface to imitate the refractive behavior of a prism. The steering angle increases as the applied voltage increases. Two dimensional beam steering is also successfully achieved by stacking two devices in orthogonal positions. The broadband feature is demonstrated using two collinear green and red laser beams.

©2009 Optical Society of America

**OCIS codes:** (010.1080) Adaptive optics; (230.2090) Electro-optical device; (010.3310) Laser beam transmission.

---

## References and links

1. S. A. Reza, and N. A. Riza, "A liquid lens-based broadband variable fiber optical attenuator," *Opt. Commun.* **282**(7), 1298–1303 (2009).
2. L. J. Hornbeck, "128 × 128 deformable mirror device," *IEEE Trans. Electron Devices* **ED 30**(5), 539–545 (1983).
3. L. Sun, J. H. Kim, C. H. Jang, D. C. An, X. J. Lu, Q. J. Zhou, J. M. Taboada, R. T. Chen, J. J. Maki, S. N. Tang, H. Zhang, W. H. Steier, C. Zhang, and L. R. Dalton, "Polymeric waveguide prism-based electro-optic beam deflector," *Opt. Eng.* **40**(7), 1217–1222 (2001).
4. B. D. Duncan, P. J. Bos, and V. Sergan, "Wide-angle achromatic prism beam steering for infrared countermeasure applications," *Opt. Eng.* **42**(4), 1038–1047 (2003).
5. P. F. McManamon, T. A. Dorschner, D. L. Corkum, L. J. Friedman, D. S. Hobbs, M. Holz, S. Liberman, H. Q. Nguyen, D. P. Resler, R. C. Sharp, and E. A. Watson, "Optical Phased Array Technology," *Proc. IEEE* **84**(2), 268–298 (1996).
6. S. Gauza, C. H. Wen, S. T. Wu, N. Janarthanan, and C. S. Hsu, "Super high birefringence isothiocyanato biphenyl-bistolane liquid crystals," *Jpn. J. Appl. Phys.* **43**(No. 11A), 7634–7638 (2004).
7. P. F. McManamon, "Agile Nonmechanical Beam Steering," *Opt. Photonics News* **17**(3), 24–29 (2006).
8. N. R. Smith, D. C. Abeyasinghe, J. W. Haus, and J. Heikenfeld, "Agile wide-angle beam steering with electrowetting micropisms," *Opt. Express* **14**(14), 6557–6563 (2006).
9. H. A. Pohl, "The motion and precipitation of suspensoids in divergent electric fields," *J. Appl. Phys.* **22**(7), 869–871 (1951).
10. C. C. Cheng, C. A. Chang, and J. A. Yeh, "Variable focus dielectric liquid lens," *Opt. Express* **14**(9), 4101–4106 (2006).
11. H. Ren, and S. T. Wu, "Variable focus dielectric liquid droplet lens," *Opt. Express* **15**(10), 5931–5936 (2007).
12. C. C. Cheng, and J. A. Yeh, "Dielectrically actuated liquid lens," *Opt. Express* **15**(12), 7140–7145 (2007).
13. H. Ren, H. Xianyu, S. Xu, and S. T. Wu, "Adaptive dielectric liquid lens," *Opt. Express* **16**(19), 14954–14960 (2008).
14. H. A. Haus, and J. R. Melcher, "Electromagnetic fields and energy," Chap. 11, [http://web.mit.edu/6.013\\_book/www/chapter11/11.9.html](http://web.mit.edu/6.013_book/www/chapter11/11.9.html)
15. H. D. Tholl, "Novel laser beam steering technique," *Technologies for Optical Countermeasures III*, *Proc. SPIE* **6397**, 639708 (2006).

---

## 1. Introduction

A beam steering device without moving parts has potential applications in emerging optical technologies. Controllable delivery of optical beams or other guided modes to a desired direction or location is crucial to any optical system for telecommunications [1], military, and other industrial applications. The most common method for steering a laser beam is the use of mechanically controlled mirrors [2]. These systems are usually bulky, slow speed, and lack of agility due to the inertia when driving the mirrors. The other well-known steering device, acousto-optic modulator, has limited application due to the cost, resolution, and reliability

issues. Some other devices without moving parts include electro-optic prism array within a polymer waveguide [3], achromatic doublet prisms [4], liquid crystal-based optical phased arrays [5–7], and liquid modulated via electrowetting [1,8]. A broadband variable fiber optical attenuator using the changing radius of a liquid lens was proposed [1], however, the tilt angle was only about 0.35 degree. A large steering angle of  $\sim 30^\circ (\pm 15^\circ)$  was demonstrated by means of electrowetting micropillar with a high index liquid [8]. Significant advances have been made in key performance areas such as size, weight, response time, and steering angle. However, providing a polarization independent, broadband beam steering device without moving parts is still highly desirable.

In this paper, we demonstrate a novel broadband beam steering using liquid optical elements manipulated through electrophoresis. Dielectrophoresis effect was discovered in the 1950's by H. Pohl [9]. Recently, dielectrophoresis has a renewed interest because of its potential applications in manipulating microparticles, nanoparticles and cells, and in adaptive liquid lenses [10–13]. Here, we extend the feasibility to broadband beam steering. This study reports the fabrication and performance evaluation of the dielectrophoresis beam steering device. The test includes steering angle, transmittance, beam divergence, dispersion, and response time, which are important to a beam steering device. Because of the compact size, two dimensional (2D) steering is also demonstrated by stacking two devices in orthogonal directions. Therefore, this simple device can achieve 2D, broadband, polarization independent, and  $\sim 100$  ms switching speed beam steering without moving parts.

## 2. Dielectrophoresis steering device

Dielectrophoresis is a phenomenon in which a force exerts on a dielectric particle when it is subjected to a nonuniform electric field. The particle does not need to be charged for inducing the force. However, the strength of the dielectric force depends on the electrical properties of the medium and particles, such as shape and dielectric constant, as well as the electric field.

### 2.1 Operation mechanism

The main structure as depicted in Fig. 1(a) is comprised of two liquids, two ITO (Indium Tin Oxide) glass substrates and a spacer. Liquid 1 (L-1) and liquid 2 (L-2) have different refractive indexes in order to steer the incident light, and different dielectric constants to induce the dielectric force. The top ITO glass is set slanted with an angle to the bottom ITO glass to generate nonuniform electric fields. At  $V = 0$ , the interface between two liquids is horizontal, which makes the light transmits straightly through the interface. When a voltage is present, the nonuniform electric field is generated due to the different distance between two ITO glasses. A longer distance causes a lower electric field (left); and a shorter distance results in a higher electric field (right). Let us assume L-2 has a larger dielectric constant than L-1. In a voltage-on state, L-2 will move toward the higher electric field region and squeeze L-1 to the right. Thus the interface between two liquids becomes slanted and the light will be deflected by the tilted interface, as depicted in the right side of Fig. 1(a).

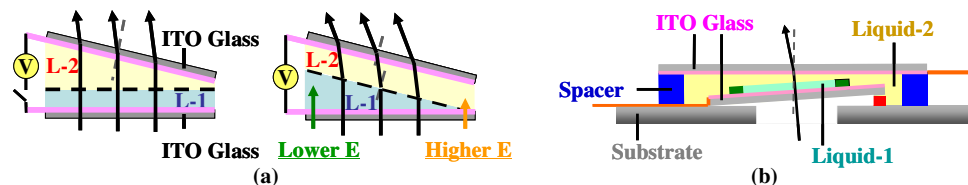


Fig. 1. (a) Illustration of the beam steering by the tilted interface between two liquids due to the dielectric force. (b) The proposed beam steering device structure.

The force acting on the interface could be estimated through the force density ( $F$ ) [14]:

$$\vec{F} = \frac{\epsilon_0}{2} (\epsilon_1 - \epsilon_2) \nabla (E \cdot E), \quad (1)$$

where  $\epsilon_0$ ,  $\epsilon_1$ , and  $\epsilon_2$  represent the dielectric constant of the free space, liquid-1, and liquid-2, respectively, and  $E$  denotes the electric field on the interface between liquid-1 and liquid-2. From Eq. (1), the dielectric constant difference between two liquids and electric field gradient are crucial to the dielectric force density. The direction of the force depends on whether ( $\epsilon_1 - \epsilon_2$ ) is positive or negative, which determines the tilt direction and angle of the interface.

## 2.2 Device structure and fabrication

To prove concept, we constructed a beam steering device as shown in Fig. 1(b). To begin fabrication, a 0.7 mm height pad (the red block in Fig. 1(b)) was placed on the substrate, with a hole (6 mm in diameter) in the center. Then the bottom ITO glass (8 × 8 mm) was mounted onto the substrate with ITO side facing up and one edge of the ITO glass is sustained by the pad to slant the glass. After that, a squared polymer dam (0.5 mm in thickness) was attached upon the bottom glass to form a squared pool for liquid-1, denoted by the green blocks in Fig. 1(b). It is important to make sure that the polymer frame is fully stuck on to the glass with no crevice because the function of the polymer frame is to wall off L-1 from L-2. Next, a spacer of 1.8 mm thick was adhered to the substrate, as represented by the blue blocks in Fig. 1(b). In order to generate nonuniform electric fields in one direction only, the coplanarity of the spacer should be well controlled. Nonuniformity in second direction would cause a nonuniform dielectric force in two directions and curve the interface, resulting in beam distortion. Otherwise, the coplanarity of the polymer dam also induces the same distortion effect as the spacer does. Afterwards, we filled L-1 into the green dam and sealed the rest space with L-2. Due to the gravity effect, L-1 should have a larger density than L-2 for easily staying beneath L-2 during both fabrication and operation. At last, we put the top ITO glass on top of the spacer.

The tilt angle of the bottom glass is ~5 degrees and the total thickness of the device is ~2 mm. Optical fluid (SL-5267) was chosen as liquid-1 and DI-water was chosen as liquid-2. Table 1 lists the physical properties of the two employed liquids. To conveniently apply a voltage to the device, we stuck a copper conductive tape onto the ITO glass beforehand.

**Table 1. Physical properties of liquid-1 and liquid-2.**

<b>Material</b>	<b>Dielectric Constant</b>	<b>Refractive Index</b>	<b>Density (g/cm<sup>3</sup>)</b>	<b>Color</b>
Liquid-1	4.6	1.67	1.2	Clear
Liquid-2	80	1.33	1.0	Clear

## 2.3 Electric field analysis

Because the dielectric force is strongly dependent on the electric field, we conducted electric field simulations in order to investigate the optimal structure dimension, such as the tilt angle for bottom glass and predicting the deformation shape of the interface between two liquids. Figure 2(a) shows the geometrical model for the electric field simulation. Two liquids and the polymer dam are modeled, while the slant angle is the main factor for the simulation. Although a larger angle induces a stronger electric field gradient and dielectric force, but it also increases the total thickness of the device. After having analyzed the results and prepared some prototypes, we chose the tilt angle to be 5 degrees. The simulated electric field distribution of liquid-1 is presented in Fig. 2(b). Higher electric field is found at the right, which causes liquid-2 to move toward right side and pressing the right interface down. Under the ideal condition, there should be no interaction between the edge of interface and the edge of polymer dam. Thus, the interface should keep flat during deformation, as denoted by the blue dashed lines in Fig. 2(b). However, from experiment we found that the edge of the liquids' interface is fixed to the edge of the polymer dam which results in wave-like interface profile, as the red solid line in Fig. 2(b) shows. Therefore, only the central region of the interface is flat which is useful for steering the incident light and keeping a good beam quality after steering.



Fig. 2. (a) Device geometry for the electric field simulation. (b) Simulated electric field distribution of liquid-1 and shape of the interface between two liquids in a voltage-on state. The blue dashed lines represent the ideal shape of the interface and the red solid line represents the actual shape of the interface.

### 3. Device performance

The functional requirements for a beam steering device are steering angle, resolution, divergence, aperture, spectral range, and throughput [15]. To characterize the performance of our beam steering device, we conducted several measurements and tests.

#### 3.1 Steering angle

Figure 3(a) depicts the experimental setup for measurements. A He-Ne laser ( $\lambda = 633$  nm) was used as a probing beam. An ac voltage (200 Hz square waves) up to  $V_{\text{rms}} = 180$  volts was applied to the copper conductive tape. As the voltage increases, the displacement ( $D$ ) gradually increases. Based on the measured  $D$ , we can calculate the steering angle through  $\tan(\theta) \sim D/L$ . In our experiment,  $L = 660$  mm. Figure 3(b) shows the measured steering angle. At  $180 V_{\text{rms}}$ , the displacement is 10.1 mm and the steering angle is  $\sim 0.87$  degree. The steering angle increases as the voltage increases, and grows rapidly in the high voltage regime where the induced electric field is stronger. This structure was designed to achieve a 4-degree steering angle. However, because the edge of the interface got stuck to the edge of polymer dam, the driving voltage was increased and the interface was curved. As a result, the observed steering angle was only  $\sim 0.87$  degree. We could increase the voltage to achieve a larger steering angle, but the high voltage could cause breakdown to the ITO electrode. Moreover, the distorted beam by the high voltage makes the measurement of spot center more difficult.

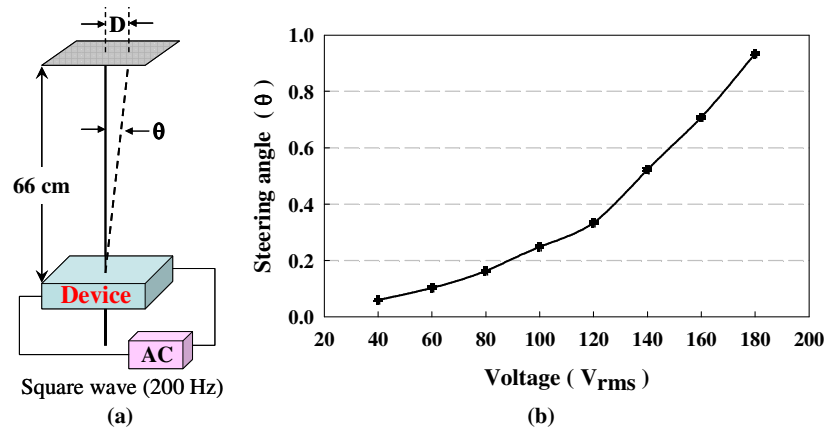


Fig. 3. (a) Setup for measuring steering angle. (b) Experimental results of steering angle vs. voltage.

#### 3.2 Beam size

As abovementioned, the edge of liquids' interface interacts with the edge of polymer dam, which affects the profile of the interface and the divergence of the beam. Thus, it is important to test the beam size variation while the light passing through the device. The setup is the

same as shown in Fig. 3(a). Figure 4(a) shows the original spot coming from the light source and projected to the screen directly. The spot size is  $\sim 2$  mm. The beam spot transmitting through the central region of the interface is shown in Fig. 4(b). Although the beam size does not change much, the spot shape is slightly distorted. When the light departed farther from the central region of the interface, shown in Fig. 4(c), distortion and divergence are more severe.

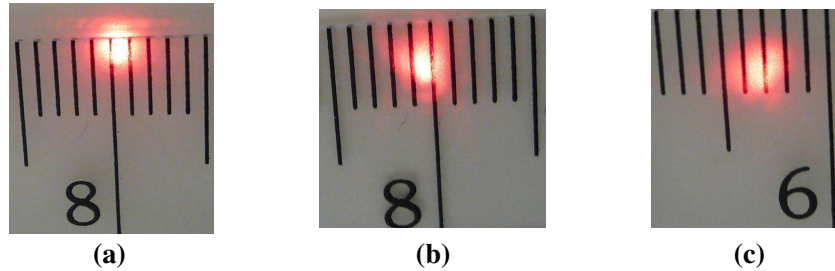


Fig. 4. (a) Laser spot without passing through the device. (b) Laser spot transmitting through the central region of the interface. (c) Laser spot transmitting through the interface farther away from the central region.

### 3.3 Dispersion of broadband steering

Because our device has prism-like structure, material dispersion (wavelength-dependent refractive index) would cause different colors to refract at different angles. We also investigated the broadband performance of our beam steering device. To easily observe the dispersion of the beam, two laser light sources, red ( $\lambda = 633$  nm) and green ( $\lambda = 532$  nm), were collinearly aligned and a screen was set at  $\sim 3$  m from the device. First, two beams were aligned without passing through the device, shown in Fig. 5(a). The spot size is  $\sim 1$  cm. Next, the beam steering device was placed in the beam path (at  $V = 0$ ) and the dispersion was observed as Fig. 5(b) shows. The color dispersion was observed and the two beams were separated by  $\sim 5.8$  mm (called dispersion distance), corresponding to  $\sim 0.1$  degree between two beams. In a voltage-on state, the dispersion distance keeps the same throughout the entire steering range.

We analyzed the dispersion phenomena using a commercial software called TracePro<sup>®</sup>. The simulated dispersion distance is  $\sim 4$  mm. The difference between simulation and experiment could result from the structure variation due to fabrication errors. However, it is indeed a broadband device in the visible spectral range.

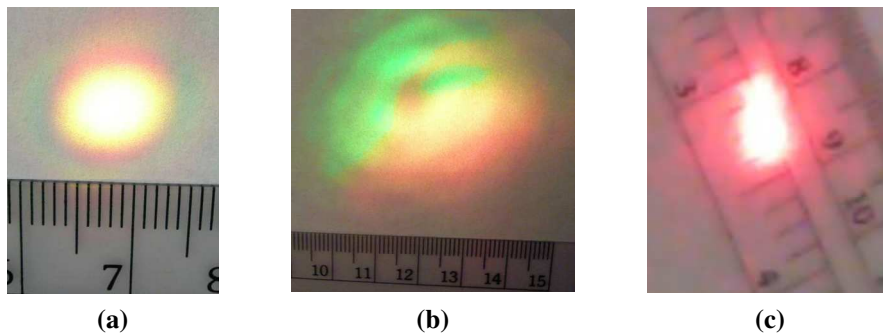


Fig. 5. (a) Beam spot combining red and green lasers. (b) Light dispersion by the device. (c) Demo of 2D beam steering by dielectrophoresis. ([Media 1](#))

### 3.4 Two dimensional steering

Due to the simple structure, easy fabrication process, and cost effective materials, two devices were fabricated and stacked together. For parallel stacking, the steering angle is doubled.

While the two devices were stacked perpendicularly, 2D steering is achieved. To visually observe the 2D beam steering, a movie for independently controlling the two orthogonal devices was recorded in Fig. 5(c). A He-Ne laser beam was used in this demo. The driving voltage was varied from  $V = 0$  to  $150 V_{\text{rms}}$ . Although the hand-made device is primitive, it clearly shows the 2D beam steering principle.

The response time of the beam steering device was measured under  $V = 110 V_{\text{rms}}$  (200 Hz square waves). The measured rise time was 339 ms and the fall time 145 ms. The total transmittance of the lens system was  $\sim 70\%$  at  $\lambda = 633$  nm, including two ITO glass substrates and two liquids; all the glass surfaces did not have anti-reflection coatings. In principle, this beam steering device can be extended to infrared, say  $\lambda = 1.55$   $\mu\text{m}$ . The key requirement is to choose liquids with good transparency in the wavelength range of interest because the DI-water and optical fluid we employed have some isolated absorptions above 1  $\mu\text{m}$ .

#### 4. Discussion and conclusion

The edge interaction, mentioned in Sec. 2.3, between the interface and the polymer dam causes the planar issue to the interface between two liquids, which affects the beam quality of the device, especially in high voltage driving. At  $V = 0$ , the entire interface is flat, but the flat region is reduced as the voltage increases. From experiments, the 2-mm spot still keeps in good shape at  $V < 120 V_{\text{rms}}$ , which means  $\sim 50\%$  of the prism interface remains flat. However, the shape of the spot is distorted when  $V > 150 V_{\text{rms}}$ . To minimize the distortion, it is better to use two liquids with the same and high surface tension, which could decrease the interface friction with the polymer dam and also improve the response time of the device. Enlarging the area of two liquids' interface is another method to improve the beam quality. However, extending the interface leads to a larger volume of the device and a higher driving voltage for this tilted prism structure.

In this study, a tilted continuous electrode was introduced to generate the gradient electric field in one direction. Therefore, the device steers the light beam to positive direction only and the gradient of electric field is dependent on the slanted angle. If we replace the top planar electrode with discrete stripe line electrodes, similar to those used in Ref. 5, the electric field gradient could be manipulated by the applied voltage to each line. Thus, both positive and negative steering directions can be achieved and steering angle doubled. Moreover, the two ITO substrates could be set parallel, which not only simplifies the device structure but also reduces the device thickness.

The total dimension of our device is about 15 mm  $\times$  15 mm and 5 mm in thickness, but the main structure without the substrate is  $\sim 2$  mm thick. To achieve a larger steering angle, several devices could be stacked together. For instance, to obtain  $4^\circ$  steering angle one could stack 5 devices together and the total thickness is  $\sim 10$  mm. However, the disadvantages associated with this approach are lower transmittance, beam walk-off, and reduced effective aperture. Therefore, the stripe line approach is preferred.

Technical issues such as driving voltage, beam quality, and response time remain to be addressed. However the device has the potential for simple fabrication, broadband and 2D beam steering, polarization independence, simple control circuits, and cost effectiveness.